

## Fabrication and mechanical properties of SiC reinforced reaction-bonded silicon nitride based ceramics

Hai-Long Hu<sup>a,b</sup>, Dong-Xu Yao<sup>a</sup>, Yong-Feng Xia<sup>a</sup>, Kai-Hui Zuo<sup>a</sup>, Yu-Ping Zeng<sup>a,\*</sup>

<sup>a</sup>State Key Lab of High Performance Ceramics and Superfine Microstructure Shanghai Institute of Ceramics, Chinese Academy of Sciences, Shanghai 200050, China

<sup>b</sup>Graduate University of Chinese Academy of Sciences, Beijing 100864, China

Received 3 June 2013; received in revised form 28 July 2013; accepted 5 September 2013

Available online 13 September 2013

### Abstract

SiC reinforced  $\text{Si}_3\text{N}_4$  based ceramics were fabricated via nitridation of silicon, and the influence of SiC addition on the microstructure and mechanical properties of the as-prepared  $\text{Si}_3\text{N}_4/\text{SiC}$  ceramics were investigated. With SiC addition increase,  $\beta\text{-Si}_3\text{N}_4$  grains growth was inhibited and equiaxed  $\text{Si}_3\text{N}_4$  grains increased. This can be attributed to grain-boundary pinning effect due to SiC dispersion, resulting in finer  $\beta\text{-Si}_3\text{N}_4$  grains with high aspect ratio. After nitridation and post-sintering at 1750 °C for 2 h,  $\text{Si}_3\text{N}_4/\text{SiC}$  composites with flexural strength of 614 MPa, young's modulus of 263 GPa, hardness of 14.3 GPa were obtained with 10 wt% SiC addition. Compared with pure  $\text{Si}_3\text{N}_4$  ceramics, the fracture toughness was also improved, reaching the peak value of 3.45  $\text{MPa m}^{1/2}$  at the SiC fraction of 10 wt%. This can be accounted for the phenomena of crack deflection and bridging.

© 2013 Elsevier Ltd and Techna Group S.r.l. All rights reserved.

**Keywords:** A. Reaction-bonded; B. Reinforced; C.  $\text{Si}_3\text{N}_4/\text{SiC}$  ceramics

### 1. Introduction

Nano or submicron SiC particle reinforced  $\text{Si}_3\text{N}_4$  ceramics has attracted wide attention owing to their notable properties, such as high hardness, superior flexural strength, excellent creep resistance, favorable oxidation as well as benign corrosion [1–4].

For improving the mechanical properties, considerable research has been done to prepare silicon nitride for its structure applications. The improved mechanical properties have been tailored by incorporating the second phase (TiC, TiN, SiC, etc.) to optimize the grain size and aspect ratio of grains [5]. J. H. Shin prepared SiC/ $\text{Si}_3\text{N}_4$  composite ceramics with improved mechanical properties in terms of increasing SiC content up to 30 wt% by using spark plasma sintering method, while the fracture toughness increased up to 20 wt% SiC addition and then decreased with further SiC addition [6]. M. Yoshimura achieved flexural strength further improvement by developing  $\text{Si}_3\text{N}_4/\text{TiN}$  composite ceramics [7]. Niihara

et al. [1] prepared 25 vol% SiC/ $\text{Si}_3\text{N}_4$  nanocomposite with a flexural strength above 1.5 GPa by using amorphous Si–C–N powders, whose high strength could be still maintained up to 1400 °C.

Generally,  $\text{Si}_3\text{N}_4/\text{SiC}$  composites have been prepared by hot-pressing [8,9] or gas pressure sintering [10] or self-propagating combustion synthesis [11]. Reaction-bonded process via nitridation of silicon powder is also a favorable route to prepare composite ceramics with suitable advantages including simple process, near-net shaping and low fabrication cost [12–14]. By incorporating the second phase, the reaction-bonded  $\text{Si}_3\text{N}_4$  based composite ceramics could achieve desirable mechanical properties, which are available to be used in structural applications such as valves, ball bearings, cutting tools, etc.

This aim of the work is to improve mechanical properties of reaction-bonded  $\text{Si}_3\text{N}_4$  ceramics by incorporating submicron-sized SiC. The  $\text{Si}_3\text{N}_4/\text{SiC}$  composites were prepared via nitridation of silicon powder at 1450 °C, using Si and SiC as starting powders, then post-sintering at 1750 °C. The dependences of phase composition, microstructure, as well as mechanical properties on the content of SiC were investigated.

\*Corresponding author. Tel.: +86 21 52415203; fax: +86 21 52413903.

E-mail address: [yuping-zeng@mail.sic.ac.cn](mailto:yuping-zeng@mail.sic.ac.cn) (Y.-P. Zeng).

## 2. Experimental procedure

### 2.1. Preparation

Commercially available silicon powder (purity  $\geq 99.9\%$  wt%;  $d_{50}=1.3\ \mu\text{m}$ ; Peixian Tiannayuan Silicon Materials Co. Ltd., Jiangsu, China),  $\alpha$ -SiC (0.5  $\mu\text{m}$ , with a purity of 99.4% in mass, Weifang Kaihua Silicon Carbide Micro-Powder Co., Ltd., Weifang, China),  $\text{Y}_2\text{O}_3$  (5.0  $\mu\text{m}$ ; purity  $\geq 99.99\%$  wt%; Yuelong Company, Shanghai, China) and  $\alpha$ - $\text{Al}_2\text{O}_3$  (99.9% purity, an average particle size of 0.6  $\mu\text{m}$ , Wusong Chemical Fertilizer Factory, Shanghai, China). The compositions of SiC/Si were calculated to make theoretical final phase composition of  $\text{Si}_3\text{N}_4/\text{SiC}$  with SiC content of 0%, 5%, 10% and 20% by weight, designated as sample SN0, SN5, SN10 and SN20, respectively. Four mixture series were prepared from the starting materials of Si and SiC.  $\text{Y}_2\text{O}_3$  and  $\text{Al}_2\text{O}_3$  were used as sintering additives, whose total amount was 15 wt% with weight ratio of  $\text{Y}_2\text{O}_3:\text{Al}_2\text{O}_3:(\text{Si}+\text{SiC})=6:9:100$ . The mixtures were ball-milled in ethanol for 24 h. After vacuum drying and sieving through 100 mesh screen, 2.5 g of powder mixture was uniaxially pressed in a stainless steel die under the pressure of 10 MPa. Then the samples were cold-isostatically pressed at a pressure of 200 MPa. The nitridation of the green bodies was conducted in a graphite resistance furnace with heating rate of  $10\ ^\circ\text{C}/\text{min}$  to  $1100\ ^\circ\text{C}$ , then temperature increased to  $1450\ ^\circ\text{C}$  at  $10\ ^\circ\text{C}/\text{h}$  and kept for 2 h to nitridation under a positive high-purity nitrogen pressure of 5 KPa. The samples were then placed in a furnace to post-sintering and the sintering was conducted at  $1750\ ^\circ\text{C}$  with 2 h hold under a nitrogen pressure of 0.6 MPa.

### 2.2. Characterization

The extent of nitridation was determined by the ratio of the weight gain. According to the following reaction Eq. (1), the theoretical weight gain is 66.7%. Crystalline phases of the sintered specimens were determined by X-ray diffractometry (XRD; D/MAX-RBX, Rigaku, Osaka, Japan) with  $\text{CuK}_\alpha$  radiation.



The specimens were machined into rectangles bars with a dimension of  $3.0\ \text{mm} \times 4.0\ \text{mm} \times 36.0\ \text{mm}$  to measure the flexural strength via the three-point bending test (Instron5566, INSTRON, Norwood, MA); the support distance of 30.0 mm and a cross-head speed of 0.5 mm/min were used. The open porosity and bulk density were determined by the Archimedes method using distilled water as medium. The microstructures of the nitrided body and post-sintered samples were characterized by observing the fracture surface, which was coated with a thin layer of gold, using scanning electron microscopy (SEM; JEOLJSM-6390, Tokyo, Japan). Cross sections were corroded in molten alkali NaOH with 30 s in  $450\ ^\circ\text{C}$ . The corroded surfaces were also observed by SEM. TEM (JEM-2100F, JEOL) combined with an energy-dispersive X-ray spectroscopy (EDS) was used to characterize the microstructure of the sample. Vickers Hardness (TUKON-2100B) was measured at 5 Kg load for 15 s, while

fracture toughness was calculated from measurements of the crack length by using the equation given by Niihara et al [15]. And HR-SEM (FEI, RiLi S-4800) was used to characterize the crack propagation after the completion of Vickers hardness for sample SN10.

## 3. Results and discussion

### 3.1. Phase composition and microstructures of the $\text{Si}_3\text{N}_4/\text{SiC}$ composites

Fig. 1 shows the XRD patterns of sintered  $\text{Si}_3\text{N}_4/\text{SiC}$  composite ceramics with various contents of SiC. After nitridation, without SiC addition, Si powder was changed into  $\text{Si}_3\text{N}_4$ ,  $\alpha$ - $\text{Si}_3\text{N}_4$  was the major phase,  $\beta$ - $\text{Si}_3\text{N}_4$  was the minor phase and no apparent intergranular phase was detected. The extent of nitridation can be influenced by many factors, such as compact density, nitriding temperature and so on. The internal volume expansion of Si to  $\text{Si}_3\text{N}_4$  could close the internal pore network in the compacts, which would prevent from the penetration of the nitrogen gas into the internal of the green body leading to the decrease of the nitridation degree of Si particles [16]. Meanwhile, there could be a little residual Si in the sintered samples below the detection limit of XRD analysis. In this experiment, the extent of nitridation for SN0, 5, 10 and 20 was 86.60%, 93.6%, 94.2% and 94.6%, respectively. The relative density of green compacts slightly increased from SN0 to SN20. SiC can act as grog addition to maintain an open pore structure, which was favorable for the compaction of silicon particles. It was revealed that the addition of the second phase (like SiC or BN) could promote the nitridation of Si powders and made contribution to the increase of relative density, as shown in B. Yuan's research [17].

After post-sintering at  $1750\ ^\circ\text{C}$  for 2 h, XRD patterns showed that the major phase in all samples was  $\beta$ - $\text{Si}_3\text{N}_4$ , SiC and  $\text{Y}_2\text{Si}_3\text{O}_3\text{N}_4$  are minor phases, and there was no  $\alpha$ - $\text{Si}_3\text{N}_4$  phase detected in all the samples, which indicated that  $\alpha$ - $\text{Si}_3\text{N}_4$  has already transferred into  $\beta$ - $\text{Si}_3\text{N}_4$  phase at sintering temperature. As SiC content increased from 0 wt% to 20 wt%, the XRD diffraction intensity of  $\beta$ - $\text{Si}_3\text{N}_4$  tended to steadily strengthen, especially with 10 wt% SiC addition, which implied that SiC addition resulted in the promotion of crystallization of  $\beta$ - $\text{Si}_3\text{N}_4$ .

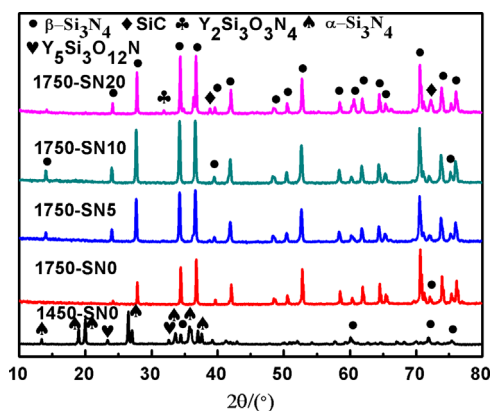


Fig. 1. XRD patterns of  $\text{Si}_3\text{N}_4/\text{SiC}$  ceramics nitrided at  $1450\ ^\circ\text{C}$  and then post-sintered at  $1750\ ^\circ\text{C}$  with contents of 0 wt%, 5 wt%, 10 wt% and 20 wt% SiC.

grains. And the XRD diffraction peak intensity of SiC increased with increasing SiC addition was also observed in Shin's [6] research. The degree of crystallization at this temperature may

be closely related with nucleation sites and surface energy of  $\beta$ - $\text{Si}_3\text{N}_4$  due to the higher energy of  $\text{Si}_3\text{N}_4$ –SiC interfaces compared with  $\text{Si}_3\text{N}_4$ – $\text{Si}_3\text{N}_4$  interfaces [18]. It was reported

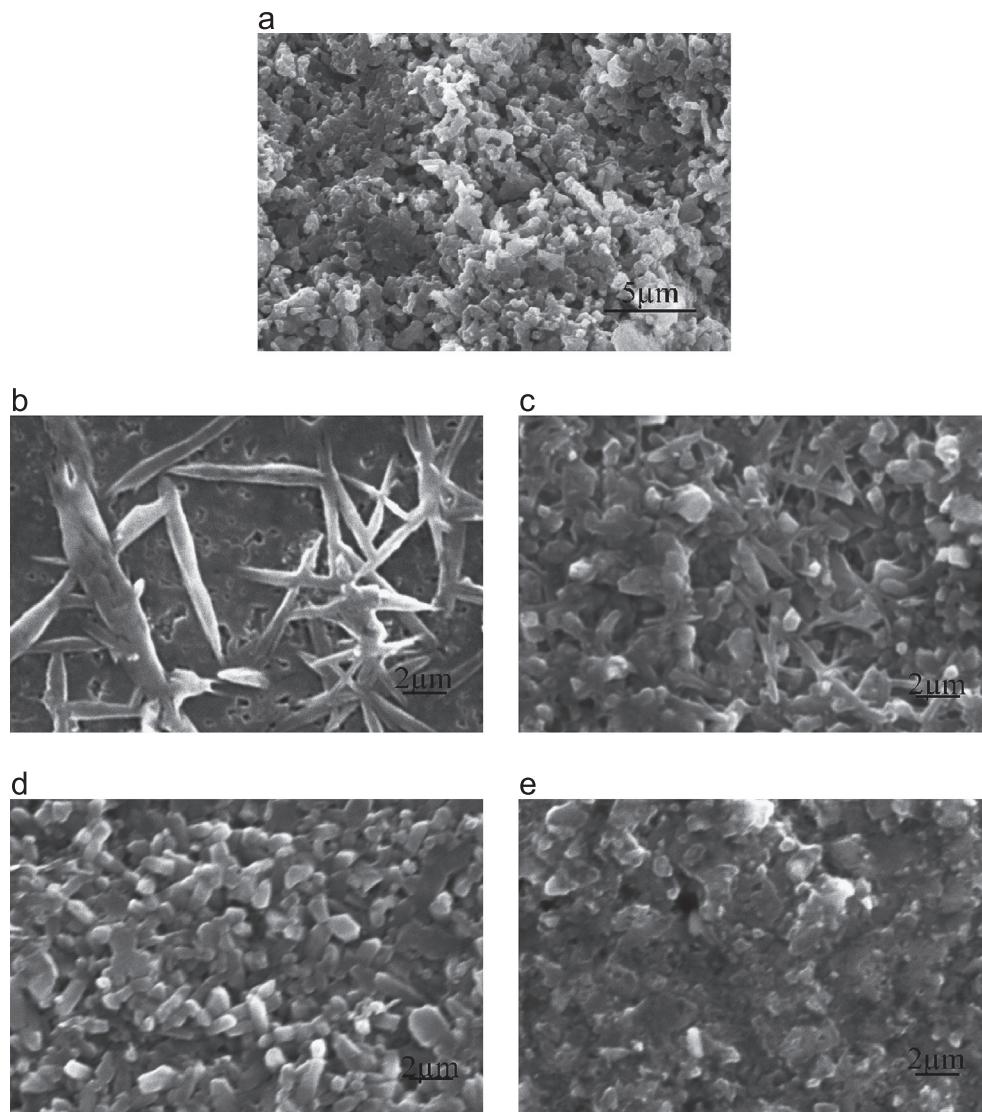


Fig. 2. SEM micrographs of  $\text{Si}_3\text{N}_4/\text{SiC}$  ceramics with SiC dispersion ranging from 0 wt% to 20 wt%. Fracture morphology: (a) SN0, 1450 °C; Eroded surfaces: (b) SN0, 1750 °C; (c) SN5, 1750 °C; (d) SN10, 1750 °C and (e) SN20, 1750 °C.

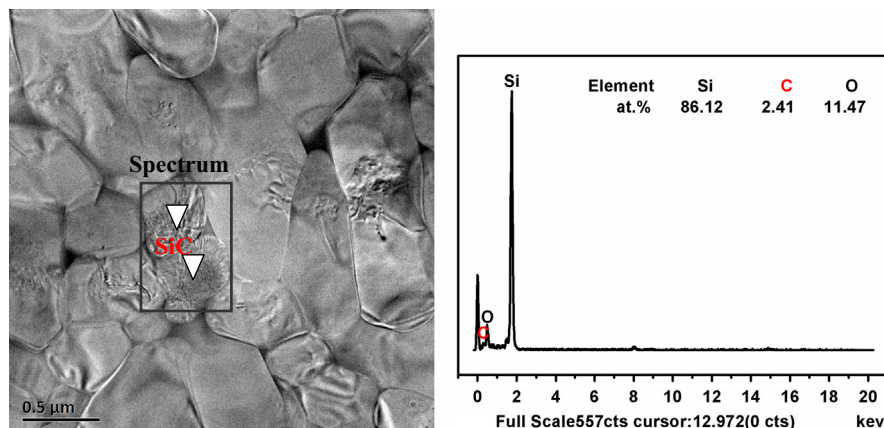


Fig. 3. TEM image of SN10 with inter granular particles and energy-dispersive X-ray spectroscopy profile.



that SiC particles could be nucleation sites for  $\beta$ - $\text{Si}_3\text{N}_4$  in  $\text{Si}_3\text{N}_4/\text{SiC}$  nanocomposite [1,18].

Fig. 2 shows the fracture morphology of the specimen SN0 obtained by nitrided at  $1450^\circ\text{C}$  and the eroded surfaces of the specimens SN0, 5, 10 and 20 post-sintered at  $1750^\circ\text{C}$ . After nitridation at  $1450^\circ\text{C}$ , specimen SN0 showed granular particles with neck growth owing to the volume expansion from Si to  $\text{Si}_3\text{N}_4$ . When sintering at  $1750^\circ\text{C}$ , SEM micrographs of specimens implied that the introduction of SiC effectively restrained the growth of  $\beta$ - $\text{Si}_3\text{N}_4$  grains during the solution-precipitation process, which became even more evident for the case of SN10 and SN20 in Fig. 2(c) and (d), compared with the SN0 showing a typical bimodal microstructure composed of large elongated  $\beta$ - $\text{Si}_3\text{N}_4$  grains and small  $\beta$ - $\text{Si}_3\text{N}_4$  matrix grains. This can be attributed to grain-boundary pinning owing to SiC dispersions, as indicated in the following Fig. 3. Meanwhile, with the higher content of SiC, the aspect ratio of  $\beta$ - $\text{Si}_3\text{N}_4$  grains was higher. It was reported that the mechanical performance of the  $\text{Si}_3\text{N}_4/\text{SiC}$  composites had been substantially affected by the  $\text{Si}_3\text{N}_4$  grain sizes and their aspect ratios [19]. Yang's results further revealed that the size decrease of  $\beta$ - $\text{Si}_3\text{N}_4$  grains is an effective approach for strengthening the  $\text{Si}_3\text{N}_4/\text{SiC}$  ceramics [20]. The typical interlocked microstructure that  $\beta$ - $\text{Si}_3\text{N}_4$  grains embedded in the matrix can be clearly observed when 10 wt% SiC was incorporated from Fig. 2(d). With higher SiC content, the interlocking extent seemed to be weakened, as shown in Fig. 2(b, c, d and e). Thus, it is believed that the dispersion of SiC in the matrix can substantially improve the flexural strength of  $\text{Si}_3\text{N}_4/\text{SiC}$  ceramics.

Fig. 3 are the TEM image and energy-dispersive X-ray spectroscopy (EDS) profile of SN10. It can be found that SiC was partly dispersed at the grain boundaries of  $\beta$ - $\text{Si}_3\text{N}_4$  grains, as indicated in the white triangle. And the appearance of SiC grain in the  $\text{Si}_3\text{N}_4$  matrix could be demonstrated by EDS profile with minor content. Due to the poor sinterability, SiC remained its original size of around 500 nm, as the white triangle indicated. A crack propagated along the surface of sample SN10 after the completion of Vickers hardness, in Fig. 4. And the phenomena of crack deflection and bridging was clearly shown, which was believed to have an important role in the improvement of fracture toughness.

### 3.2. Mechanical properties of the $\text{Si}_3\text{N}_4/\text{SiC}$ composites

Fig. 5 shows the young's modulus and fracture toughness of  $\text{Si}_3\text{N}_4/\text{SiC}$  ceramics with various contents of SiC. Both of them firstly increased and then decreased as the SiC content increased. At the content of 10 wt% SiC, both of them reached the peak value of appropriate 263 GPa and  $3.45 \text{ MPa} \cdot \text{m}^{1/2}$ . In addition, the highest hardness of 14.3 GPa was also obtained at 10 wt% SiC addition. However, the toughness enhancement with SiC addition was not commonly observed in previous research [21,22]. But Yang's results revealed that increased toughness with 5 wt% SiC/ $\text{Si}_3\text{N}_4$  nanocomposites was ascribed to grain bridging by SiC particles<sup>20</sup>. Since the distance between SiC particles was much smaller than between  $\text{Si}_3\text{N}_4$  grains, small bridging zone of SiC particles behind the crack tip formed, resulting in the higher toughness. And a decrease in toughness with the increase of SiC content has been reported, owing to the decreased grain size

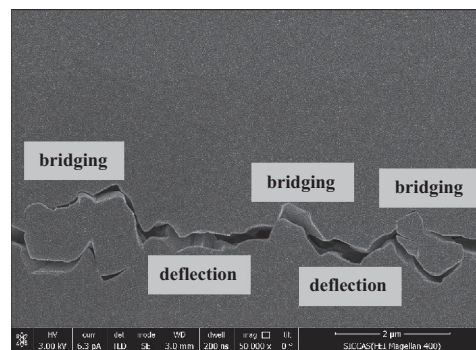


Fig. 4. HR-SEM image of toughening mechanism for SN10.

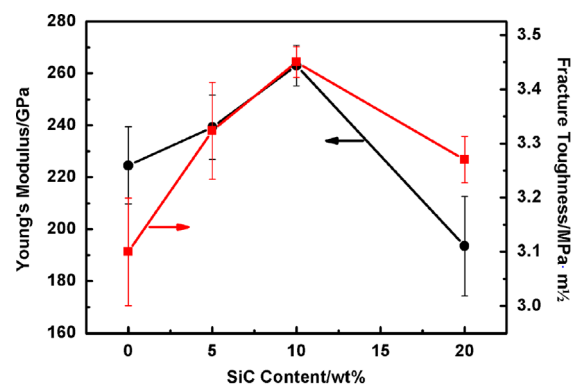


Fig. 5. Young's modulus and fracture toughness of  $\text{Si}_3\text{N}_4/\text{SiC}$  ceramics with various contents of SiC.

[23,24]. In this experiment, compared with monolithic  $\text{Si}_3\text{N}_4$  ceramics without SiC addition, the fracture toughness with SiC addition showed a slight increase. This could be explained by the interlocking morphology (Fig. 2(d)), which favored crack deflection and bridging (Fig. 4). Because the grain-boundary pinning effect of SiC resulted in finer  $\beta$ - $\text{Si}_3\text{N}_4$  grains with high aspect ratio (Fig. 3). These will do favor in the improvement of fracture toughness for ceramics. The young's modulus substantially decreased at the fraction of 20 wt%, and this can be attributed to the decreased relative density.

Fig. 6 reveals the results of flexural strength and relative density with various contents of SiC. Although the relative density was slightly decreased from about 97% to 96% with the increase of SiC content between 0 wt% and 10 wt% and the flexural strength reached the peak value of approximate 614 MPa at 10 wt% SiC, which is about 11% increment compared with monolithic  $\text{Si}_3\text{N}_4$  ceramics of 506 MPa without SiC addition. This phenomenon was in accordance with the reported research of SiC reinforced  $\text{Si}_3\text{N}_4$  ceramics, which gained highest flexural strength with SiC content of 5–30 wt% by using  $\alpha$ - $\text{Si}_3\text{N}_4$  powder and nano SiC powder [1,18,20]. Thus, with nearly the equivalent relative density, the flexural strength substantially improved, this was chiefly attributed to the inhibition of grain growth owing to the reinforced effect of SiC dispersion in the matrix. In the case of SN20, the flexural strength decreased to about 351 MPa. To a large extent, it conformed to the low relative density of 89.16%.

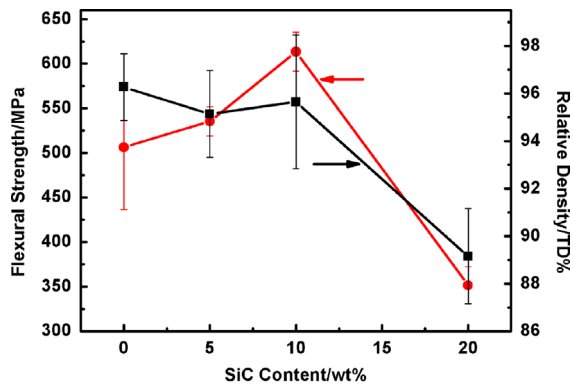


Fig. 6. Flexural strength and relative density of  $\text{Si}_3\text{N}_4/\text{SiC}$  ceramics with various contents of SiC.

#### 4. Conclusions

In this paper, SiC reinforced  $\text{Si}_3\text{N}_4$  ceramics with high flexural strength and high relative density were prepared via nitridation of Si powder with SiC as addition and  $\text{Y}_2\text{O}_3/\text{Al}_2\text{O}_3$  as sintering additives. SiC particle dispersed in the grain boundary and restrained the growth of  $\beta\text{-Si}_3\text{N}_4$  grains during the solution-precipitation process. Owing to the pinning effect of SiC,  $\text{Si}_3\text{N}_4/\text{SiC}$  ceramics with favorable mechanical properties have obtained at 10 wt% SiC, whose flexural strength, Young's modulus, hardness and fracture toughness were 614 MPa, 263 GPa, 14.3 GPa and  $3.45 \text{ MPa} \cdot \text{m}^{1/2}$ , respectively. The obtained material will bring great benefit to the application of structural engineering devices.

#### References

- [1] K. Niihara, New design concept of structural ceramics – ceramic nanocomposites, *Journal of The Ceramic Society of Japan* 99 (1991) 974–982.
- [2] M. Mitomo, N. Hirotsaki, T. Nishimura, R.J. Xie, Microstructure control in silicon nitride ceramics – a review, *Journal of The Ceramic Society of Japan* 114 (2006) 867–872.
- [3] F.L. Riley, Silicon-nitride-and-related-materials, *Journal of the American Ceramic Society* 83 (2000) 245–265.
- [4] T. Hirano, K. Niihara, Microstructure and Mechanical-Properties of  $\text{Si}_3\text{N}_4/\text{SiC}$  Composites, *Materials Letters* 22 (1995) 249–254.
- [5] G. Petzow, M. Herrmann, Silicon nitride ceramics, *Structure and Bonding* 102 (2002) 47–167.
- [6] J.H. Shin, B. Venkata, M. Kumar, J.H. Kim, S.H. Hong, Tribological properties of  $\text{Si}_3\text{N}_4/\text{SiC}$  nano-nano composite ceramics, *Journal of the American Ceramic Society* 94 (2011) 3683–3685.
- [7] M. Yoshimura, O. Komura, A. Yamakawa, Microstructure and tribological properties of nano-sized  $\text{Si}_3\text{N}_4$ , *Scripta Materialia* 44 (2001) 1517–1521.
- [8] F. Luo, D.M. Zhu, X.L. Su, W.C. Zhou, Properties of hot-pressed of  $\text{SiC}/\text{Si}_3\text{N}_4$  nanocomposites. a-structural materials properties microstructure and processing, *Materials Science and Engineering* 458 (2007) 7–10.
- [9] P. Sajgalik, M. Hnatko, P. Copan, Z. Lencses, J.L. Huang, Influence of graphite additives on wear properties of hot pressed  $\text{Si}_3\text{N}_4$  ceramics, *Journal of The Ceramic Society of Japan* 114 (2006) 1061–1068.
- [10] C. Santos, C.A. Kelly, S. Ribeiro, K. Strecker, J.V.C. Souza, O.M. M. Silva,  $\alpha\text{-SiAlON-SiC}$  composites obtained by gas-pressure sintering and hot-pressing, *Journal of Materials Processing Technology*. 189 (2007) 138–142.
- [11] C.S. Zheng, Q.Z. Yan, M. Xia, C.C. Ge, In situ preparation of  $\text{SiC}/\text{Si}_3\text{N}_4$ -NW composite powders by combustion synthesis, *Ceramics International* 38 (2012) 487–493.
- [12] F. Luo, D.M. Zhu, H. Zhang, W.C. Zhou, Properties of reaction-bonded  $\text{SiC}/\text{Si}_3\text{N}_4$  ceramics, *Materials Science and Engineering* 431 (2006) 285–289.
- [13] L. Yuan, J.K. Yu, S.W. Zhang, Fabrication of porous reaction-bonded  $\text{Si}_3\text{N}_4\text{-SiC}$  composites, *Chemical Engineering and Material Properties, Parts 1 and 2*. 391 (2012) 575–579.
- [14] J.F. Li, S. Satomi, R. Watanabe, M. Omori, T. Hirai, Fabrication and characterization of SiC rod-particulate-reinforced reaction-bonded  $\text{Si}_3\text{N}_4$  composites, *The Journal of the European Ceramic Society* 20 (2000) 1795–1802.
- [15] K. Niihara, R. Morena, D.P.H. Hasselman, Evaluation of K<sub>IC</sub> of Brittle Solids by the Indentation Method with Low Crack-to-Indent Ratios, *Journal of Materials Science Letters* 1 (1982) 13–16.
- [16] M.H. Bocanegra-Bernal, B. Matovic, Dense and near-net-shape fabrication of  $\text{Si}_3\text{N}_4$  ceramics, *Materials Science and Engineering* 500 (2009) 130–149.
- [17] B. Yuan, J.X. Liu, G.J. Zhang, Y.M. Kan, P.L. Wang, Silicon nitride/boron nitride ceramic composites fabricated by reactive pressureless sintering, *Ceramics International* 35 (2009) 2155–2159.
- [18] T.O. Jian-Feng Yang, et al., Phase transformation, microstructure and mechanical properties of  $\text{Si}_3\text{N}_4/\text{SiC}$  composite, *The Journal of the European Ceramic Society* 21 (2001) 2179–2183.
- [19] T. Hirao, and, K. Niihara, Microstructure and mechanical properties of  $\text{Si}_3\text{N}_4/\text{SiC}$  composites, *Materials Letters* 22 (1995) 249–254.
- [20] J.F. Yang, T. Sekino, Y.H. Choa, K. Niihara, Microstructure and Mechanical Properties of Sinter-Post-HIPed  $\text{Si}_3\text{N}_4\text{-SiC}$  Composites, *Journal of the American Ceramic Society* 84 (2001) 406–412.
- [21] K. Niihara, T. Hirano, A. Nakahira, K. Ishizaki, The correlation between interface structure and mechanical properties for silicon nitride based nanocomposite, in: K. Ishizaki, K. Niihara, M. Isotani, R.G. Ford (Eds.), *Grain Boundary Controlled Properties of Fine Ceramics*, Elsevier, London, U.K., 1992, pp. 103–111.
- [22] G. Sasaki, H. Nakase, K. Suganuma, T. Fujita, K. Niihara, Mechanical properties and microstructure of  $\text{Si}_3\text{N}_4$  matrix composite with nano-metre scale SiC particle, *Journal of The Ceramic Society of Japan* 100 (1992) 536–540.
- [23] I. Minato, G. Pezzotti, K. Niihara, Microstructure and fracture behaviours for  $\text{Si}_3\text{N}_4$ -based ceramics, *Journal of the Japan Society of Powder and Powder Metallurgy* 39 (1992) 1076–1079.
- [24] G. Pezzotti, M. Sasaki, Effect of a silicon carbide nano-dispersion on the mechanical properties of silicon nitride, *Journal of the American Ceramic Society* 77 (1994) 3039–3041.